

Causal Bayesian Optimization via Exogenous Distribution Learning

Shaogang Ren

shaogang-ren@utc.edu

Department of Computer Science and Engineering
University of Tennessee at Chattanooga

Xiaoning Qian

Department of Electrical and Computer Engineering
Texas A&M University

Abstract

Maximizing a target variable as an operational objective in a structural causal model is an important problem. Existing Causal Bayesian Optimization (CBO) methods either rely on hard interventions that alter the causal structure to maximize the reward; or introduce action nodes to endogenous variables so that the data generation mechanisms are adjusted to achieve the objective. In this paper, a novel method is introduced to learn the distribution of exogenous variables, which is typically ignored or marginalized through expectation by existing methods. Exogenous distribution learning improves the approximation accuracy of structural causal models in a surrogate model that is usually trained with limited observational data. Moreover, the learned exogenous distribution extends existing CBO to general causal schemes beyond Additive Noise Models (ANMs). The recovery of exogenous variables allows us to use a more flexible prior for noise or unobserved hidden variables. We develop a new CBO method by leveraging the learned exogenous distribution. Experiments on different datasets and applications show the benefits of our proposed method.

1 Introduction

Bayesian Optimization (BO) has broad applications, such as automating modern industrial processes, drug discovery, and more general synthetic biology, that require optimizing black-box objective functions [15; 3]. In many real-world problems, we have some structural knowledge of the unknown functions that can be leveraged to improve BO efficiency. CBO has been developed to utilize the structural information of the objective [2; 1; 23]. CBO combines ideas from causal inference,

uncertainty quantification, and sequential decision-making. It generalizes Bayesian Optimization, which treats the input variables of the objective function as independent, to scenarios where causal information between input variables is available [2]. CBO has been developed for optimizing medical and ecological interventions as illustrative examples [2; 1].

1.1 Approach and Contributions

In this paper, we develop a Causal Bayesian Optimization method, EXCBO. Given observation data points of a structural causal model (SCM, [19; 18]), the exogenous variable associated with each endogenous node is recovered with an encoder-decoder framework. The learned distribution of the exogenous variable is then approximated with the density of the recovered exogenous variable that is parameterized with a flexible model, e.g. Gaussian Mixture. The recovered exogenous distribution improves the surrogate model’s accuracy in the SCM approximation. Different from existing CBO methods [2; 1; 23] that typically focus on Additive Noise Models (ANMs, [11]), our method enables us to extend CBO to general causal models beyond ANMs. Our flexible surrogate model has the benefit of better causal inference regarding CBO updating.

The contributions in this paper include

- We propose a method to recover the exogenous noise variable of each endogenous node in an SCM using observational data; the exogenous distribution in each node is then learned using a flexible model that is capable of modeling multi-mode density functions;
- We develop an EXogenous distribution learning augmented Causal Bayesian Optimization algorithm (EXCBO), where the flexibility of learning exogenous distributions naturally extends the proposed CBO framework to general causal models beyond ANMs.
- We provide a theoretical study on the recovery of exogenous variables. Moreover, we give a theoretical analysis of the algorithm regret bound. Our analysis shows that the proposed EXCBO algorithm achieves sublinear cumulative regret bounds.
- Experiments have been performed to validate the benefits of exogenous distribution learning and the proposed EXCBO algorithm. Applications on epidemic dynamic model calibration and COVID-19 testing are discussed to support the proposed CBO framework.

In the following parts of this paper, Section 2 presents the background and related work; Section 3 sets up the problem studied in this paper with the introduction of the proposed CBO framework; Section 4 presents the exogenous recovery method; The proposed SCM algorithm, EXCBO, is detailed in Section 5 with theoretical analysis of EXCBO given in Section 6; Section 7 presents experimental results; Section 8 concludes the paper.

2 Background and Related Work

In this section, we give a brief review of SCM, intervention, and CBO methods.

2.1 Structural Causal Model

An SCM is denoted by $\mathcal{M} = (\mathcal{G}, \mathbf{F}, \mathbf{X}, U)$. Here \mathcal{G} is a directed acyclic graph (DAG), and $\mathbf{F} = \{f_i\}_{i=0}^d$ stands for $d + 1$ mechanisms of all variables. \mathbf{X} is the endogenous variable set, and U is the exogenous (background) variable set. Samples of the i th endogenous variable are generated with

$$X_i = f_i(\mathbf{Z}_i, U_i); \mathbf{Z}_i = \mathbf{pa}(i), U_i \sim p(U_i), \text{ for } i \in [d]. \quad (1)$$

Here $[d] = \{0, 1, \dots, d\}$. We use X_i to represent the i th variable as well as the i th node in \mathcal{G} , and $\mathbf{pa}(i)$ stands for the parents of i , and $\mathbf{ch}(i)$ is the children of node X_i regarding \mathcal{G} . In addition, we have $U_i \perp\!\!\!\perp X_i$ and $U_i \perp\!\!\!\perp U_j, \forall i \neq j$. f_i is a mapping from $\mathbb{R}^{|\mathbf{pa}(i)|+1} \rightarrow \mathbb{R}$. Moreover, \mathcal{X}_i and \mathcal{Z}_i stand for the value range of X_i and \mathbf{Z}_i , respectively. Existing CBO methods [2; 23] usually assume that the exogenous variable is an ANM [11] to the data generation mechanism, i.e., $X_i = f_i(\mathbf{Z}_i) + U_i$, with $U_i \sim \mathcal{N}(0, 1)$.

2.2 Intervention

In SCM \mathcal{M} , let \mathbf{I} be a subset of endogenous variables, i.e. $\mathbf{I} \subset \mathbf{X}$. The intervention on target \mathbf{I} is given by $\mathbf{F}_x = \{f_i | X_i \notin \mathbf{I}\} \cup \{f_j | X_j \in \mathbf{I}\}$. The intervention on variable X_j is implemented with the change of the data generation mechanism from f_i to a constant scalar. There are generally two types of interventions: hard and soft intervention. The hard intervention on target \mathbf{I} is given by $\mathbf{F}_x = \{f_i | X_i \notin \mathbf{I}\} \cup \{f_j := \alpha_j | X_j \in \mathbf{I}\}$. Here α is the realization of variables in \mathbf{I} . The do-operation [19] $do(\mathbf{X} := \alpha)$ represents the hard intervention that changes the SCM from \mathcal{M} to \mathcal{M}_α . A hard intervention on a node breaks its causal connection with its parents.

This paper focuses on the soft intervention (or imperfect intervention, [20]). Following Model-based CBO (MCBO, [23]), we introduce an action variable to each endogenous variable, i.e., $\mathbf{F}_x = \{f_i | X_i \notin \mathbf{I}\} \cup \{f_j := f_j(\mathbf{Z}_j, A_j, U_j) | X_j \in \mathbf{I}\}$. Here $\mathbf{Z}_j = \mathbf{pa}(j)$. With the soft intervention on target \mathbf{I} , the data generation mechanism becomes

$$X_i = \begin{cases} f_i(\mathbf{Z}_i, U_i), & \text{if } X_i \notin \mathbf{I} \\ f_i(\mathbf{Z}_i, A_i, U_i), & \text{if } X_i \in \mathbf{I} \end{cases}, \quad (2)$$

where A_i is the continuous action variable for X_i if $X_i \in \mathbf{I}$. Action A_i with the corresponding value range \mathcal{A}_i controls the change of the data generation mechanism of node X_i .

2.3 Function Network Bayesian Optimization

Similar to CBO, the structure of the functions in Function Network BO (FNBO, [4; 3]) is assumed to be given, and the parameters and specific form of each function are unknown. FNBO operates soft interventions and uses an expected improvement (EI) acquisition function to select actions. FNBO assumes that the system is noiseless, which could be a restrictive assumption in practice. Both FNBO and CBO belong to a broad research direction using intermediate observations from the computation of the unknown functions to improve the sample efficiency of vanilla BO algorithms [5].

2.4 Causal Bayesian Optimization

In CBO, a sequence of actions is performed to interact with an SCM \mathcal{M} . The graph structure, DAG \mathcal{G} in \mathcal{M} is given, with the edge functions $\mathbf{F} = \{f_i\}_{i=0}^d$ being fixed but unknown. Probabilistic surrogate models (typically Gaussian Processes, i.e. GPs, [24]) are implemented to search for the intervention actions in attaining the optimal objective/reward value. In [2], the authors proposed a CBO algorithm that obtains both the optimal intervention target set and the corresponding input values to reach the optimal objective value in an SCM. A dynamic CBO (DCBO) algorithm is proposed in [1], where all causal effects in the SCM \mathcal{M} are changing over time.

In MCBO [23], soft interventions are optimized to achieve the maximum target variable of an SCM. With action variables, the edge function set becomes $\mathbf{F} = \{f_i\}_{i=0}^d$ with $f_i : \mathcal{Z}_i \times \mathcal{A}_i \rightarrow \mathcal{X}_i$. Let $x_{i,t}$ denote the observation of node X_i at time step t , and $i \in [d]$, $t \in [T]$. T is the total number of time steps. At step t MCBO selects actions $a_{:t} = \{a_{i,t}\}_{i=0}^d$ and obtains observations $\mathbf{x}_{:,t} = \{x_{i,t}\}_{i=0}^d$.

The relation between the action $a_{i,t}$ and the observation is given by an additive noise model, i.e., $x_{i,t} = f_i(\mathbf{z}_{i,t}, a_{i,t}) + u_{i,t}$, $\forall i \in [d]$. At the target node d , $a_{d,t} = 0$, and $y_t = f_d(\mathbf{z}_{d,t}, a_{d,t}) + u_{d,t}$, and here y_t depends on the whole intervention vector. The action vector that maximizes the expected reward regarding the exogenous variable is \mathbf{a}^* , i.e. $\mathbf{a}^* = \arg \max_{\mathbf{a} \in \mathcal{A}} \mathbb{E}[y|\mathbf{a}]$. The GP surrogate model is implemented to learn the reward function and guide BO in optimizing y .

3 Problem Statement

This section gives the problem statement of the proposed EXCBO algorithm. Compared to existing methods, our proposed CBO framework studies more general causal models as given in (1). Following existing CBO algorithms [2; 1; 23], the DAG \mathcal{G} is assumed to be known. Similar to MCBO, our framework adopts GP surrogate models to guide the optimization of soft interventions controlled by an action vector $\mathbf{a} = \{a_i\}_{i=0}^d$ in reaching the optimal reward value. This section gives details about the problem settings studied in this paper.

3.1 Regularity Assumption

In our problem, the edges in SCM \mathcal{M} is a fixed but unknown set of functions $\mathbf{F} = \{f_i\}_{i=0}^d$ with $f_i : \mathcal{Q} \rightarrow \mathcal{X}_i$. We assume the structure of the SCM is known and the problem is causal sufficient, which means that there are no unobserved variables or confounders. We consider standard smoothness assumptions for the unknown functions f_i defining over a compact domain \mathcal{Q} [21]. For each node $i \in [d]$, we assume that $f_i(\cdot)$ belongs to a reproducing kernel Hilbert space (RKHS) \mathcal{H}_k , a space of smooth functions defined on $\mathcal{Q} = \mathcal{Z}_i \times \mathcal{A}_i \times \mathcal{U}_i$. This means that $f_i \in \mathcal{H}_{k_i}$ is induced by a kernel function $k_i : \mathcal{Q} \times \mathcal{Q} \rightarrow \mathbb{R}$. We also assume that $k_i(s, s') \leq 1$ for every $s, s' \in \mathcal{Q}$. The RKHS norm of $f_i(\cdot)$ is assumed to be bounded $\|f_i\|_{k_i} \leq \mathcal{B}_i$ for some fixed constant $\mathcal{B}_i > 0$ [23]. We further assume that \mathcal{A}_i and $\mathcal{U}_i, i \in [d]$ are compact and bounded. The intervention target set \mathbf{I} is assumed to a subset of \mathbf{X} , i.e., $|\mathbf{I}| \leq d - 1$.

3.2 CBO via Exogenous Distribution Learning

Different from ANMs in existing CBO algorithms, such as MCBO [23] briefly reviewed in Section 5, we here propose to flexibly model the mapping $f_i(\cdot)$ with introduced exogenous variables, for which we propose a new EXCBO framework for CBO through exogenous distribution learning. At step t of CBO, the relation between actions $a_{i,t}$, $u_{i,t}$ and the observation $x_{i,t}$ is given by

$$x_{i,t} = f_i(\mathbf{z}_{i,t}, a_{i,t}, u_{i,t}) \quad \forall i \in [d]. \quad (3)$$

Our surrogate model in EXCBO takes the exogenous variable U_i as the input as shown in (3) and Figure 1. In our SCMs, the exogenous variables are not simply noise in the system. We assume they are important background or environmental factors that affect the output of the SCM. Additionally, each U_i can be Gaussian or non-Gaussian and has multiple modes.

Using an example in biology, $x_{i,t}$ is the community size of a species of bacteria at time t , $u_{i,t}$ is the amount of a chemical compound in the environment that affects the growth of the bacteria but independent with other factors and unknown to us, and $a_{i,t}$ is a controllable factor, e.g. environment humidity.

Let \mathcal{R} represent the root node set. As the parent of root nodes is null, we set $\mathbf{z}_{i,t} = \mathbf{0}$, if $i \in \mathcal{R}$. Similarly, we have $a_{d,t} = 0$ at the target node d ,

$$y_t = f_d(\mathbf{z}_{d,t}, a_{d,t}, u_{d,t}).$$

Given an action vector $\mathbf{a} = \{a_i\}_{i=0}^d$ and $u = \{u_i\}_{i=0}^d$, the reward or target value is simply denoted with $y = \mathbf{F}(\mathbf{a}, u)$. The problem becomes searching for an action vector maximizing the objective:

$$\mathbf{a}^* = \arg \max_{\mathbf{a} \in \mathcal{A}} \mathbb{E}[y|\mathbf{a}], \quad (4)$$

where the expectation is taken over u . The goal of our method is to design a sequence of interventions $\{\mathbf{a}_t\}_{t=0}^T$ that achieves a high average expected reward. The learning of exogenous variable distribution provides a more accurate surrogate model given an SCM and observational data.

To analyze the convergence of our method, we study the cumulative regret over a time horizon of T :

$$R_T = \sum_{t=1}^T \left[\mathbb{E}[y|\mathbf{a}^*] - \mathbb{E}[y|\mathbf{a}_{:,t}] \right].$$

Cumulative regret bound helps us to analyze the convergence property of the algorithm. In the experiments, we use the attained objective value or reward value y as the metric to compare our method and existing algorithms. A better metric depends on the real-world application and the effectiveness of the optimized action sequence.

3.3 Motivations for Exogenous Distribution Learning

In existing CBO models, exogenous distributions are ignored or marginalized to achieve the simplicity of interventions [2; 1; 23]. As mentioned in previous sections, we propose an encoder-decoder scheme to recover the exogenous variable of each endogenous node in an SCM. The distribution of the exogenous variable (U) is approximated with the density of the recovered surrogate exogenous variable (\hat{U}) which is modeled with a flexible model, e.g. Gaussian Mixture. The recovered exogenous distribution improves the surrogate model in the approximation of the SCM. Thus different from existing methods [2; 1; 23] that typically rely on the ANM assumption, our EXCBO allows us to extend CBO to a broader scope of causal models beyond ANMs. In addition, with a more accurate surrogate model, our method could achieve improved reward and objective values.

4 Exogenous Distribution Learning

Given the observations of an endogenous node and its parents in a SCM, our method is to recover the distribution of the node's exogenous variable. The learning of the exogenous distribution is implemented with Gaussian Processes. We first focus on the exogenous distribution learning regarding one node.

4.1 Exogenous Variable Recovery for One Node

According to (2), an endogenous variable X_i either has an action variable A_i or not. To better illustrate the idea with compact notations, we use \mathbf{Z}_i to represent variable X_i 's parents and its action variable in this section (Section 4), i.e., $\mathbf{Z}_i = (\mathbf{Z}_i, A_i)$ if $X_i \in \mathbf{I}$. Hence the learning of node

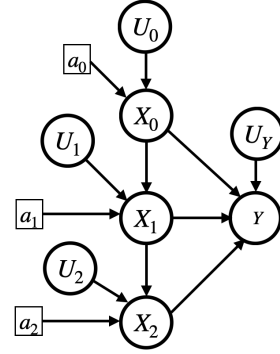


Figure 1: **EXCBO**: Causal Bayesian Optimization through exogenous distribution learning. The distribution of U_i is approximated with the density of the recovered surrogate \hat{U}_i . The EXCBO algorithm searches for the action vector \mathbf{a} that maximizes the reward Y .

X 's exogenous distortion becomes a problem of recovering U 's distribution given the observations of X and \mathbf{Z} regarding equation $X = f(\mathbf{Z}, U)$. To make our presentation concise, we have the following definition for the causal mechanism of the triplets (\mathbf{Z}, U, X) that appear as a node in an SCM.

Definition 4.1. (τ -SCM) Let X and U be one-dimensional variables, and $f()$ is the causal mechanism generating X from variables Z and U , i.e. $X = f(\mathbf{Z}, U)$. We assume $\mathbf{Z} \perp\!\!\!\perp U$, and (\mathbf{Z}, U, X, f) is defined as a τ -SCM.

In a τ -SCM, \mathbf{Z} is the parent of X , and it may be multi-dimensional; U is the exogenous variable of X . Different from the bijective generation mechanisms (BGM, [16]), $f()$ is not confined to be monotonic and invertible regarding X and U given a value of \mathbf{Z} .

The encoder-decoder framework (shown in Figure 2) is used to recover a surrogate of the exogenous variable.

Definition 4.2. (EDS) Let (\mathbf{Z}, U, X, f) be a τ -SCM. Let $\phi()$ be a regression model, $\phi() : \mathbf{Z} \rightarrow \mathcal{X}$, with mean $\mu_\phi()$ and variance $\sigma_\phi()$. We define (\hat{U}, ϕ, h, g) as encoder-decoder surrogate (EDS) model of the exogenous variable U with the encoder $h() : \mathcal{Z} \times \mathcal{X} \rightarrow \hat{\mathcal{U}}$, $\hat{U} := h(\mathbf{Z}, X) := \frac{X - \mu_\phi(\mathbf{Z})}{\sigma_\phi(\mathbf{Z})}$; and the decoder $g() : \mathcal{Z} \times \hat{\mathcal{U}} \rightarrow \mathcal{X}$, $X := g(\mathbf{Z}, \hat{U})$.

With the observations of X and its parent \mathbf{Z} , our method learns the encoder $h()$ that aims to recover the value of U , i.e., $\hat{u} = h(\mathbf{z}, x)$; our algorithm also learns the decoder $x = g(\mathbf{z}, \hat{u})$ that provides us a surrogate model of the mechanism $f()$.

Theorem 4.1 shows that the surrogate values of the exogenous variable U can be recovered from the observations of node X under the decomposable generation mechanism (DGM) assumption of f , i.e. $X = f(\mathbf{Z}, U) = f_a(\mathbf{Z}) + f_b(\mathbf{Z})f_c(U)$.

Theorem 4.1. Let (\mathbf{Z}, U, X, f) be a τ -SCM, and (\hat{U}, ϕ, h, g) is an EDS surrogate of the exogenous variable U . We assume that $f()$ is differentiable and has a decomposable structure as $X = f(\mathbf{Z}, U) = f_a(\mathbf{Z}) + f_b(\mathbf{Z})f_c(U)$, and $f_b(\mathbf{Z}) \neq 0$. Then with a constant a , $\hat{U} = a(f_c(U) - \mathbb{E}[f_c(U)])$, $\mathbb{E}[\hat{U}] = 0$, and $\hat{U} \perp\!\!\!\perp \mathbf{Z}$.

Remark 4.1. We use the distribution of $\hat{U} = \mathbf{s}(U) = h(\mathbf{Z}, X)$, i.e. $p(\hat{U})$, to represent $p(U)$ in the surrogate model. With the decomposable assumption on $f()$, a τ -SCM is counterfactually identifiable.

DGM is significantly different from the ANM [11] mechanism given by $X = f(\mathbf{pa}(X)) + U$, which is a linear monotonic function of U and widely used by many existing BO and CBO methods. In our DGM, $f_c()$ can be any continuous function, including nonlinear, non-convex, and non-monotonic function classes regarding U . Moreover, $f_b(\mathbf{Z})$ can be any continuous function as long as $f_b(\mathbf{Z}) \neq 0$. The last term of a DGM, i.e. $f_b(\mathbf{Z})f_c(U)$, indicates that given a fixed value of the parent Z , the generated variable X 's variance is not only determined by U but also by the value of \mathbf{Z} . Therefore, with $f_b(\mathbf{Z})$ DGM represents a larger class of mechanisms that both U and \mathbf{Z} affect the variance of the generated variable X . These features substantially extend the identification of exogenous variable U to much broader nonlinear and non-monotonic data-generation mechanism classes compared to ANM (linear) and BGM (monotonic). Figure 3 gives the relationship between different mechanisms.

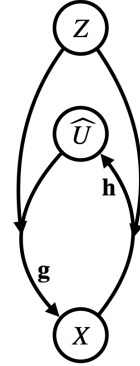


Figure 2: Structure in one τ -SCM node. \mathbf{Z} is the parent set of X , and our algorithm learns an encoder h and a decoder g so that the surrogate $\hat{U} = h(\mathbf{Z}, X)$ and $X = g(\mathbf{Z}, \hat{U})$.

In our surrogate model, $f()$ is approximated with the learned $g()$ and \hat{u} , i.e., $x = f(\mathbf{z}, u) = g(\mathbf{z}, \hat{u}) = g(\mathbf{z}, \mathbf{s}(u))$. With the monotonic assumption on $f()$, we can extend the EDS framework to BGMs by following the analysis in [14; 16; 17; 8].

Theorem 4.2. *Let (\mathbf{Z}, U, X, f) be a τ -SCM. $\forall \mathbf{z} \in \mathcal{Z}$, $f(\mathbf{z}, \cdot)$ is differentiable and strictly monotonic regarding $u \in \mathcal{U}$. Let (\hat{U}, ϕ, h, g) be an EDS surrogate of U . We further assume that $\hat{U} \perp\!\!\!\perp \mathbf{Z}$. Then $\hat{U} = h(\mathbf{Z}, X)$ is a function of U , i.e., $\hat{U} = \mathbf{s}(U)$, and $\mathbf{s}()$ is an invertible function.*

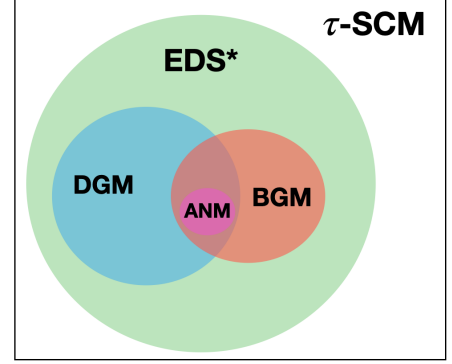


Figure 3: Scopes of different mechanisms.

The proofs of Theorem 4.1 and Theorem 4.2 can be found in the Appendix. The proposed exogenous variable surrogate \hat{U} and the encoder $h()$ work under either the DGM conditions in Theorem 4.1 or the BGM [16] conditions in Theorem 4.2.

This means that the proposed EDS model is suitable for ANMs, DGMs, and BGMs. For a BGM model, we need to enforce independence between \hat{U} and \mathbf{Z} , i.e. $\hat{U} \perp\!\!\!\perp \mathbf{Z}$, to recover U according to Theorem 4.2. It could be achieved by adding an independence regularization on both variables, which may introduce additional computation costs.

We use EDS^* to represent the τ -SCMs that are counterfactually identifiable by using EDS with or without the $\hat{U} \perp\!\!\!\perp \mathbf{Z}$ condition and Figure 3 gives the scopes of different mechanisms including EDS^* . If $f()$ does not meet the DGM and the BGM assumptions, the learned $\hat{U} = \frac{X - \mu_\phi(\mathbf{Z})}{\sigma_\phi(\mathbf{Z})}$ may not be independent of the parent variable \mathbf{Z} , and we may not get an accurate surrogate model for the SCM. It may decrease the possibility of attaining the optimal objective value of y using limited training samples.

4.2 Implementation of Exogenous Distribution Learning

There are multiple ways to implement the encoder-decoder framework in Figure 2, e.g., via Variational Auto-Encoder (VAE) [12]. To make the implementation simple, we implement both the encoder and decoder using Gaussian Process regression models based on EDS definition 4.2. For a node with an action variable A , the decoder becomes $g() : \mathcal{Z} \times \mathcal{A} \times \hat{\mathcal{U}} \rightarrow \mathcal{X}$, the encoder becomes $h() : \mathcal{Z} \times \mathcal{A} \times \mathcal{X} \rightarrow \hat{\mathcal{U}}$, and $\phi() : \mathcal{Z} \times \mathcal{A} \rightarrow \mathcal{X}$. Here $g()$ and $\phi()$ are implemented with Gaussian Process regression models [24].

We use a Gaussian Mixture model to fit the recovered distribution of \hat{U} , i.e. $p(\hat{U})$. We use $p(\hat{U})$ to replace $p(U)$ in the computing of the probabilistic surrogate objective. For the nodes in SCM \mathcal{M} , let $\mathbf{G} = \{g_i\}_{i=0}^d$, and $\mathbf{H} = \{h_i\}_{i=0}^d$.

5 CBO with Exogenous Distribution Learning

In this section, we present the EXCBO algorithm, describing the probabilistic model and acquisition function used.

5.1 Statistical Model

In our model, the function f_i that generates variable X_i is learned through g_i , and $X_i = g_i(\mathbf{Z}_i, A_i, \hat{U}_i)$. We use Gaussian Processes [24] to learn the surrogate of g_i , i.e., \tilde{g}_i . For $i \in [d]$, let $\mu_{g,i,0}$ and $\sigma_{g,i,0}$

denote the prior mean and variance function for each f_i , respectively.

Following [9], at time t , let $\tilde{\mathbf{G}}$ be the statistically plausible function set of \mathbf{G} , i.e., $\tilde{\mathbf{G}} = \{\tilde{g}_i\}_{i=0}^d$. Similarly, the plausible model of \mathbf{H} is denoted $\tilde{\mathbf{H}} = \{\tilde{h}_i\}_{i=0}^d$. Moreover, at step t , the observation set is $\mathcal{D}_t = \{\mathbf{z}_{:,1:t}, a_{:,1:t}, x_{:,1:t}\}$. The posterior of g_i with the input of node i , $(\tilde{\mathbf{z}}_i, \tilde{a}_i, \tilde{u}_i)$, is given by

$$\begin{aligned}\tilde{g}_{i,t}(\tilde{\mathbf{z}}_i, \tilde{a}_i, \tilde{u}_i) &\sim \mathcal{GP}(\mu_{g,i,t-1}, \sigma_{g,i,t-1}); \\ \mu_{g,i,t-1} &= \mu_{g,i,t-1}(\tilde{\mathbf{z}}_i, \tilde{a}_i, \tilde{u}_i); \quad \sigma_{g,i,t-1} = \sigma_{g,i,t-1}(\tilde{\mathbf{z}}_i, \tilde{a}_i, \tilde{u}_i).\end{aligned}$$

Then $\tilde{x}_{i,t} = \tilde{g}_{i,t}(\tilde{\mathbf{z}}_i, \tilde{a}_i, \tilde{u}_i)$ denotes observations from one of the plausible models. Here $\tilde{u}_i \sim p(\hat{U}_i)$ in the sampling of the learned distribution of \hat{U}_i .

Given an observation (\mathbf{z}_i, a_i, x_i) at node i , the exogenous recovery $\hat{u}_i = h_i(\mathbf{z}_i, a_i, x_i) = \frac{x_i - \mu_{\phi,i}(\mathbf{z}_i, a_i)}{\sigma_{\phi,i}(\mathbf{z}_i, a_i)}$. At time step t , the posterior of ϕ_i with the input of node i , (\mathbf{z}_i, a_i) , is given by

$$\tilde{\phi}_{i,t}(\mathbf{z}_i, a_i) \sim \mathcal{GP}(\mu_{\phi,i,t-1}(\mathbf{z}_i, a_i), \sigma_{\phi,i,t-1}(\mathbf{z}_i, a_i)) \quad (5)$$

Therefore, $\tilde{u}_i = \tilde{h}_{i,t}(\mathbf{z}_i, a_i, x_i) = \frac{x_i - \mu_{\phi,i,t-1}(\mathbf{z}_i, a_i)}{\sigma_{\phi,i,t-1}(\mathbf{z}_i, a_i)}$. According to the definition of $h()$ in Theorem 4.1, $h()$ also follows a Gaussian Process, i.e. $h_{i,t}(\mathbf{z}_i, a_i, x_i) \sim \mathcal{GP}(\mu_{h,i,t-1}, \sigma_{h,i,t-1})$. This GP is defined by $\tilde{\phi}_{i,t}()$ which is sampled with (5). Different from $g_i()$, the observations of the input (\mathbf{Z}_i, A_i, X_i) for $h_i()$ are only required at the training time, and we only need to sample the learned $p(\hat{U}_i)$ to get value \hat{u}_i for model prediction or model sampling.

5.2 Acquisition Function

Algorithm 1 describes the proposed method solving (4). In iteration t , it uses GP posterior belief of y to construct an upper confidence bound (UCB, [7]) of y :

$$\text{UCB}_{t-1}(\mathbf{a}) = \mu_{t-1}(\mathbf{a}) + \beta_t \sigma_{t-1}(\mathbf{a}). \quad (6)$$

Here

$$\mu_{t-1}(\mathbf{a}) = \mathbb{E}[\mu_{g,d,t-1}(\tilde{\mathbf{z}}_d, \tilde{a}_d, \tilde{u}_d)] ; \quad \sigma_{t-1}(\mathbf{a}) = \mathbb{E}[\sigma_{g,d,t-1}(\tilde{\mathbf{z}}_d, \tilde{a}_d, \tilde{u}_d)],$$

where the expectation is taken over $p(\hat{U})$. In (6), β_t controls the tradeoff between exploration and exploitation of Algorithm 1. The UCB-based algorithm is a classic strategy that is widely used in BO and stochastic bandits [13; 21]. The proposed algorithm adapts the ‘‘optimism in the face of uncertainty’’ (OFU) strategy by taking the expectation of the UCB as part of the acquisition process.

5.3 Algorithm

Let $k_{g,i}, k_{\phi,i}, \forall i \in [d]$ represent the kernel functions of g_i and ϕ_i . The proposed EXCBO algorithm is summarized by Algorithm 1. In each iteration, a new sample is observed according to the UCB values. Then the posteriors of \mathbf{G} and \mathbf{H} are updated with the new dataset. The next section gives a theoretical analysis of the algorithm.

6 Theoretical Study

Algorithm 1 EXCBO

Input: $k_{g,i}, k_{\phi,i}, \forall i \in [d]$ **Result:** Intervention actions $a_i, \forall i \in [d]$ **for** $t = 1$ **to** T **do** Find \mathbf{a}_t by optimizing the acquisition function, $\mathbf{a}_t \in \arg \max \text{UCB}_{t-1}(\mathbf{a})$; Observe samples $\{\mathbf{z}_{i,t}, x_{i,t}\}_{i=0}^d$ with the action sequence \mathbf{a}_t and update \mathcal{D}_t ; Use \mathcal{D}_t to update posteriors $\{\mu_{\phi,i,t}, \sigma_{\phi,i,t}^2\}_{i=0}^d$ and sample the exogenous surrogate $\{\hat{u}_{i,t}\}_{i=0}^d$; Use $\mathcal{D}_t \cup \{\hat{u}_{i,t}\}_{i=0}^d$ to update the decoder posteriors $\{\mu_{g,i,t}, \sigma_{g,i,t}^2\}_{i=0}^d$;**end for**

This section describes the convergence guarantees for EXCBO using soft interventions. Our analysis follows the theoretical study in [23] and shows that EXCBO has a sublinear cumulative regret bound.

In DAG \mathcal{G} over $\{X_i\}_0^d$, let N be the maximum distance from a root to X_d , i.e., $N = \max_i \text{dist}(X_i, X_d)$. Here $\text{dist}(\cdot, \cdot)$ is a measure of the edges in the longest path from X_i to the reward node X_d . Let M denote the maximum number of parents of any variables in \mathcal{G} , $M = \max_i |\text{pa}(i)|$. Let L_t be a function of L_g , L_{σ_g} , and N . With Assumptions C.1- C.3 in the Appendix, the following theorem bounds the performance of EXCBO in terms of cumulative regret.

Theorem 6.1. *Consider the optimization problem in (4), with the SCM satisfying Assumptions C.1- C.3, where \mathcal{G} is known but \mathbf{F} is unknown. Then with probability at least $1 - \alpha$, the cumulative regret of Algorithm 1 is bounded by*

$$R_T \leq \mathcal{O}(L_T M^N d \sqrt{T \gamma_T}).$$

Here $\gamma_T = \max_t \gamma_{i,T}$ denote the maximum information gain at time T . This maximum information gain is commonly used in many Bayesian Optimizations [21]. Many common kernels, such as linear and squared exponential kernels, lead to sublinear information gain in T , and it results in an overall sublinear regret for EXCBO [23]. The proof of Theorem 6.1 and further analysis can be found in the Appendix.

The analysis in this paper focuses on the DGM mechanisms. To extend the analysis to BGMs, we need to consider the computation cost involving the independence penalization on variables \hat{U} and \mathbf{Z} . For mechanisms beyond DGMs and BGMs, we conjecture that the surrogate approximation accuracy may decrease, but the convergence rate may not decrease a lot.

7 Experimental Study

This section presents experimental comparisons of the proposed EXCBO and existing algorithms.

7.1 Baselines

We compare EXCBO against three algorithms: UCB, EICF, and MCBO, where UCB is a conventional method of BO [7]; EICF [3] is the composite function method of BO; MCBO [23] is the CBO method discussed in previous sections. Unlike other methods, MCBO relies on neural networks along with GPs to model uncertainty. All algorithms are implemented with Python and BoTorch [6], and we use the implementations of UCB, EICF, and MCBO in the package published with [23; 22]. The initial observation size for MCBO is the default value from the package [22], which is $2(|A| + 1)$, and $|A|$ is the number of action variables. For other methods, the initial sample size is in the range

of [5, 20]. We use four different random seeds to run all the algorithms to obtain the means and standard derivations of the reward values. All the experiments are conducted on an HPC cluster with CentOS 7 OS, 48-core nodes, and 10 GB of requested memory.

7.2 Alpine2 Dataset

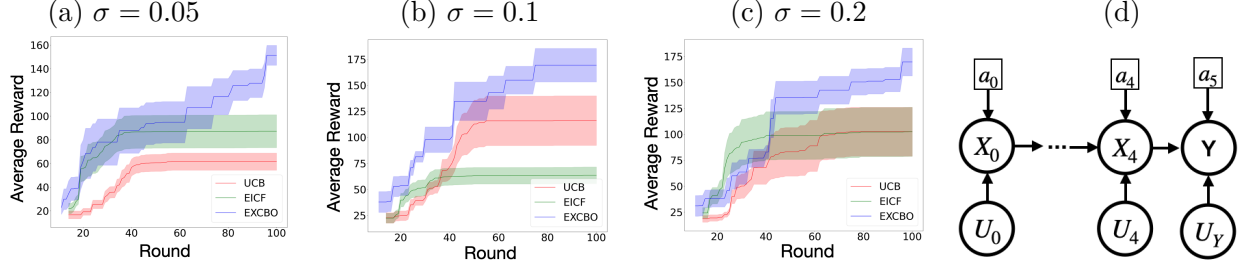


Figure 4: (a-c): Results of Alpine2 at different noise levels; (d): Alpine2 graph structure.

We study the algorithms using the Alpine2 dataset. There are six endogenous nodes in the Alpine2 dataset as shown in Figure 4-(d). The exogenous distributions for X and Y are Gaussian Mixture models with two components, i.e.,

$$p(U) = w_1 \mathcal{N}(\mu_1, c_1 \sigma) + w_2 \mathcal{N}(\mu_2, c_2 \sigma), \quad w_1, w_2, c_1, c_2 > 0. \quad (7)$$

Due to the excessively long computing time used by MCBO, we have two baselines in this set of experiments, i.e., UCB and EICF. The results of Alpine2 are shown in Figures 4-(a-c). As shown in the plots, our EXCBO performs the best on all three noise levels. It proves the effectiveness and benefits of the proposed EXCBO method.

7.3 Epidemic Model Calibration

We test EXCBO on an epidemic model calibration by following the setup in [4]. In this model, as shown in Figure 5-(c), $I_{i,t}$ represents the fraction of the population in group i that are “infectious” at time t ; $\beta_{i,j,t}$ is the rate of the people from group i who are “susceptible” have close physical contact with people in group j who are “infectious” at time t . We assume there are two groups, and infections resolve at a rate of γ per period. The number of infectious individuals in group i at the start of the next time period is $I_{i,t+1} = I_{i,t}(1 - \gamma) + (1 - I_{i,t}) \sum_j \beta_{i,j,t} I_{j,t}$. We assume each $I_{i,t}$ has an observation noise $U_{i,t}$. The model calibration problem is that given limited noisy observations of $I_{i,t}$ s, how to efficiently find the $\beta_{i,j,t}$ values in the model. The reward is defined as the negative mean square error (MSE) of all the $I_{i,t}$ observations as the objective function to optimize. In this model, $\beta_{i,j,t}$ s are the action variables.

Figure 5-(a-b) visualize the results at the noise levels with $\sigma = 0.1$ and $\sigma = 0.3$. The noise is added with two models as in (7). As shown in Figure 5-(a-b), our EXCBO always performs better than state-of-the-art model calibration methods in both cases, and our method has a faster convergence rate compared to the baselines. With the capability to recover and learn the exogenous distributions, our method is more robust and stable in this application scenario.

7.4 Pooled Testing for COVID-19

We further compare EXCBO and existing methods using the COVID-19 pooled testing problem [4]. The graphical structure is given by Figure 6-(c). In Figure 6-(c), I_t is the fraction of the population

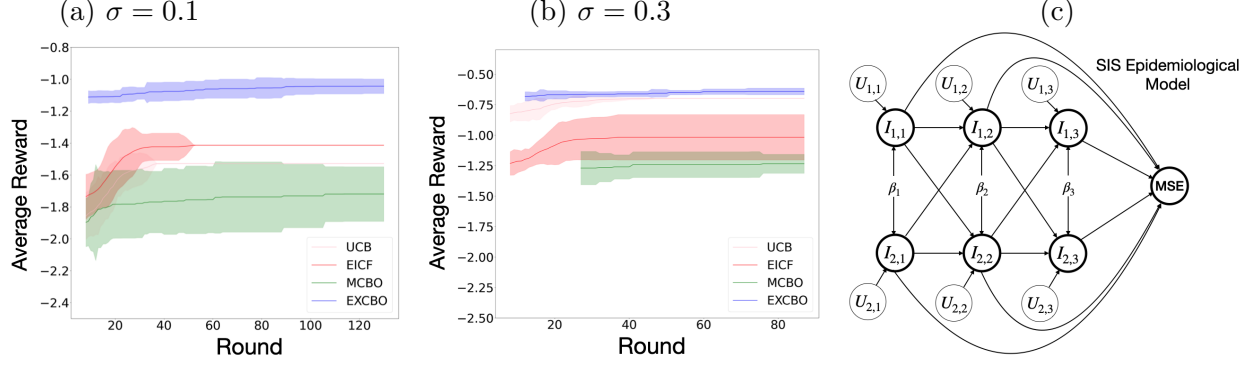


Figure 5: (a-b): Results of epidemic model calibration; (c): Graph structure for epidemic model calibration.

that is infectious at time t ; R_t is the fraction of the population that is recovered and cannot be infected again, and time point $t \in \{1, 2, 3\}$. The additional fraction $S_t = 1 - I_t - R_t$ of the population is susceptible and can be infected. During each period t , the entire population is tested using a pool size of x_t . The loss L_t , incorporates the costs resulting from infections, testing resources used, and individuals isolated at period t . The objective is to choose pool size x_t to minimize the total loss $\sum_t L_t$. Therefore, x_t s are the action variables/nodes that the algorithms try to optimize to achieve lower costs. Figure 6-(a-b) gives the optimization results from different methods, where the reward $y = -\sum_t L_t$. The proposed method EXCBO achieves the best rewards at both noise levels $\sigma = 0.2$ and $\sigma = 0.4$. MCBO’s inferior results on this dataset might be because of the over-fitting issue of the neural networks. The experimental results on different datasets show that the learned exogenous distributions improve EXCBO’s capability to reach the optimal reward values.

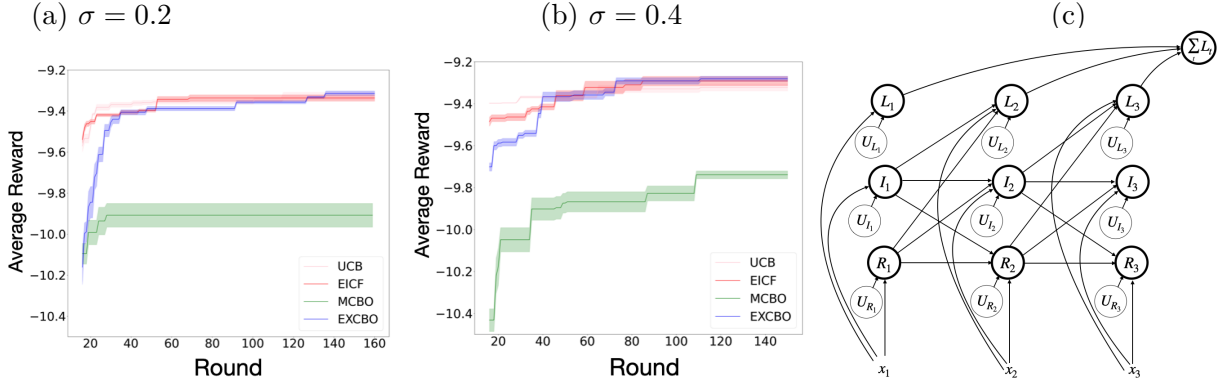


Figure 6: (a-b): Results of COVID-19 pooled testing optimization; (c): Graph structure for COVID-19 pooled testing problem.

8 Conclusions

We propose a novel Causal Bayesian Optimization algorithm, EXCBO, that approximately recovers the endogenous variables in a structured causal model. With the recovered exogenous distribution, our method naturally improves the surrogate model’s accuracy in the approximation of the SCM. Furthermore, the recovered exogenous variables may enhance the surrogate model’s capability in causal inference and hence improve the reward values attained by EXCBO. We additionally provide theoretical analysis on both exogenous variable recovery and the algorithm’s

cumulative regret bound. Experiments on multiple datasets show the algorithm’s soundness and benefits.

References

- [1] Virginia Aglietti, Neil Dhir, Javier González, and Theodoros Damoulas. Dynamic causal bayesian optimization. *Advances in Neural Information Processing Systems (NeurIPS)*, 34:10549–10560, 2021.
- [2] Virginia Aglietti, Xiaoyu Lu, Andrei Paleyes, and Javier González. Causal bayesian optimization. In *International Conference on Artificial Intelligence and Statistics (AISTats)*, pages 3155–3164. PMLR, 2020.
- [3] Raul Astudillo and Peter Frazier. Bayesian optimization of composite functions. In *International Conference on Machine Learning (ICML)*, pages 354–363. PMLR, 2019.
- [4] Raul Astudillo and Peter Frazier. Bayesian optimization of function networks. *Advances in neural information processing systems (NeurIPS)*, 34:14463–14475, 2021.
- [5] Raul Astudillo and Peter I Frazier. Thinking inside the box: A tutorial on grey-box bayesian optimization. In *2021 Winter Simulation Conference (WSC)*, pages 1–15. IEEE, 2021.
- [6] Maximilian Balandat, Brian Karrer, Daniel R. Jiang, Samuel Daulton, Benjamin Letham, Andrew Gordon Wilson, and Eytan Bakshy. BoTorch: A Framework for Efficient Monte-Carlo Bayesian Optimization. In *Advances in Neural Information Processing Systems (NeurIPS)*, 2020.
- [7] Eric Brochu, Vlad M Cora, and Nando De Freitas. A tutorial on bayesian optimization of expensive cost functions, with application to active user modeling and hierarchical reinforcement learning. *arXiv preprint arXiv:1012.2599*, 2010.
- [8] Patrick Chao, Patrick Blöbaum, and Shiva Prasad Kasiviswanathan. Interventional and counterfactual inference with diffusion models. *arXiv preprint arXiv:2302.00860*, 2023.
- [9] Sayak Ray Chowdhury and Aditya Gopalan. Online learning in kernelized markov decision processes. In *The 22nd International Conference on Artificial Intelligence and Statistics (AISTats)*, pages 3197–3205. PMLR, 2019.
- [10] Sebastian Curi, Felix Berkenkamp, and Andreas Krause. Efficient model-based reinforcement learning through optimistic policy search and planning. *Advances in Neural Information Processing Systems (NeurIPS)*, 33:14156–14170, 2020.
- [11] Patrik Hoyer, Dominik Janzing, Joris M Mooij, Jonas Peters, and Bernhard Schölkopf. Nonlinear causal discovery with additive noise models. In *Advances in neural information processing systems (NeurIPS)*, 2008.
- [12] Diederik P Kingma and Max Welling. Auto-encoding variational bayes. In *The 2nd International Conference on Learning Representations (ICLR)*, 2014.
- [13] Tor Lattimore and Csaba Szepesvári. *Bandit algorithms*. Cambridge University Press, 2020.

- [14] C. Lu, B. Huang, K. Wang, J. M. Hernández-Lobato, K. Zhang, and B. Schölkopf. Sample-efficient reinforcement learning via counterfactual-based data augmentation. In *Offline Reinforcement Learning - Workshop at the 34th Conference on Neural Information Processing Systems (NeurIPS)*, 2020.
- [15] Jonas Moćkus. On bayesian methods for seeking the extremum. In *Optimization Techniques IFIP Technical Conference: Novosibirsk, July 1–7, 1974*, pages 400–404. Springer, 1975.
- [16] Arash Nasr-Esfahany, Mohammad Alizadeh, and Devavrat Shah. Counterfactual identifiability of bijective causal models. In *International Conference on Machine Learning (ICML)*. PMLR, 2023.
- [17] Arash Nasr-Esfahany and Emre Kiciman. Counterfactual (non-)identifiability of learned structural causal models. *arXiv preprint arXiv:2301.09031*, 2023.
- [18] Judea Pearl. Causal diagrams for empirical research. *Biometrika*, 82(4):669–688, 1995.
- [19] Judea Pearl. *Causality*. Cambridge University Press, 2009.
- [20] Jonas Peters, Dominik Janzing, and Bernhard Schölkopf. *Elements of causal inference: foundations and learning algorithms*. The MIT Press, 2017.
- [21] Niranjan Srinivas, Andreas Krause, Sham Kakade, and Matthias Seeger. Gaussian process optimization in the bandit setting: no regret and experimental design. In *International Conference on International Conference on Machine Learning (ICML)*, page 1015–1022, 2010.
- [22] Scott Sussex, Anastasiia Makarova, and Andreas Krause. MCBO. <https://github.com/ssethz/mcbo>, 2023.
- [23] Scott Sussex, Anastasiia Makarova, and Andreas Krause. Model-based causal bayesian optimization. In *International Conference on Learning Representations (ICLR)*, 2023.
- [24] Christopher KI Williams and Carl Edward Rasmussen. *Gaussian processes for machine learning*. MIT press Cambridge, MA, 2006.

A Additional Remarks

A.1 Limitations

There are two main limitations of this work. Firstly, the proposed exogenous variable recovery method (EDS) only works under the DGM or BGM assumptions. DGMs and BGMs are a small portion of the whole data generation mechanisms. We leave the empirical and theoretical study of EDS on non-DGM and non-BGM mechanisms to future works. Secondly, empirically, our EXCBO method may require more training samples to achieve superior performance when the variance of the noise or exogenous variable increases. It means that datasets with stronger noise or additional uncertainty may require more training samples to recover the exogenous distributions. But eventually, our method could outperform existing methods given enough data samples.

A.2 Impact Statements

As a new causal Bayesian optimization framework, EXCBO may help reduce the required training samples for more efficient and cost-effective decision-making, which may have broader impacts in many science and engineering applications, such as future pandemic preparedness with better-calibrated epidemic dynamic models as illustrated in the paper. However, if misused, the societal consequences of designing new systems or materials with unforeseen future threats has to be taken into consideration with caution.

B Analysis on Exogenous Variable Recovery

B.1 Proof of Theorem 4.1

Before we prove Theorem 4.1, we present a similar result for ANMs [11].

Theorem B.1. *Let (X, \mathbf{Z}, U, f) be a τ -SCM. Let $\rho() : \mathcal{X} \times \mathcal{Z} \rightarrow \mathbb{R}^1$ be a predefined function regarding X and \mathbf{Z} , and $\phi()$ be a regression model with $\phi() : \mathcal{Z} \rightarrow \rho(\mathcal{X}, \mathcal{Z})$. We define an encoder function $h() : \mathcal{Z} \times \mathcal{X} \rightarrow \hat{\mathcal{U}}$ with $\hat{\mathcal{U}} := h(\mathbf{Z}, X) := \rho(X, \mathbf{Z}) - \phi(\mathbf{Z})$. The decoder is $g() : \mathcal{Z} \times \hat{\mathcal{U}} \rightarrow \mathcal{X}$, i.e., $X = g(\mathbf{Z}, \hat{\mathcal{U}})$. Let $\rho()$ maps the values of X and \mathbf{Z} to an additive function of \mathbf{Z} and U , i.e., $\rho(X, \mathbf{Z}) = \rho_1(\mathbf{Z}) + \rho_2(U)$. Then $\hat{\mathcal{U}} = h(\mathbf{Z}, X) = \rho_2(U) - \mathbb{E}[\rho_2(U)]$, and $\hat{\mathcal{U}} \perp\!\!\!\perp \mathbf{Z}$.*

Proof. As $\phi(\mathbf{z})$ is an optimal approximation of $\rho(X, \mathbf{z})$, with $\mathbf{Z} \perp\!\!\!\perp U$, we have

$$\begin{aligned} \phi(\mathbf{z}) &= \mathbb{E}[\rho(X, \mathbf{z})] = \mathbb{E}[\rho_1(\mathbf{z}) + \rho_2(U)] = \int (\rho_1(\mathbf{z}) + \rho_2(u))p(u)du \\ &= \rho_1(\mathbf{z}) + \mathbb{E}[\rho_2(U)]. \end{aligned}$$

Thus, the decoder becomes

$$\begin{aligned} h(\mathbf{z}, x) &= \rho(x, \mathbf{z}) - \phi(\mathbf{Z} = \mathbf{z}) \\ &= \rho_1(\mathbf{z}) + \rho_2(u) - \rho_1(\mathbf{z}) - \mathbb{E}[\rho_2(U)] \\ &= \rho_2(u) - \mathbb{E}[\rho_2(U)]. \end{aligned}$$

Therefore, $\hat{\mathcal{U}} = h(\mathbf{Z}, X) = \rho_2(U) - \mathbb{E}[\rho_2(U)]$ is a function of U , and $h(\mathbf{Z}, X) \perp\!\!\!\perp \mathbf{Z}$, i.e., $\hat{\mathcal{U}} \perp\!\!\!\perp \mathbf{Z}$. \square

Example B.1. *For an ANM [11] model $X = f(\mathbf{Z}) + U$, we have $\rho(X, \mathbf{Z}) = X$, $\rho_1(\mathbf{Z}) = f(\mathbf{Z})$, and $\rho_2(U) = U$, then $\hat{\mathcal{U}} = h(\mathbf{Z}, X) = U - \bar{U}$.*

Example B.2. For a model $X = 2Ze^{-U} - e^{-Z}$, we have $\rho(X, Z) = \log(X + e^{-Z})$, $\rho_1(Z) = \log(2Z)$, and $\rho_2(U) = -U$, then $\hat{U} = h(Z, X) = -U + \bar{U}$.

Example B.1 shows that the exogenous variable in any ANM model is identifiable. In practice, variable X 's generation mechanism $f()$ is generally unknown, and it is hard to propose a general form function $\rho()$ that can perform on any $f()$ s and transform them to ANMs.

Theorem 4.1 Let (\mathbf{Z}, U, X, f) be a τ -SCM, and (\hat{U}, ϕ, h, g) is an EDS surrogate of the exogenous variable U . We assume that $f()$ is differentiable and has a decomposable structure as $X = f(\mathbf{Z}, U) = f_a(\mathbf{Z}) + f_b(\mathbf{Z})f_c(U)$, and $f_b(\mathbf{Z}) \neq 0$. Then with a constant a , $\hat{U} = a(f_c(U) - \mathbb{E}[f_c(U)])$, $\mathbb{E}[\hat{U}] = 0$, and $\hat{U} \perp\!\!\!\perp \mathbf{Z}$.

Proof. $\forall \mathbf{z} \in \mathcal{Z}$, as $\phi(\mathbf{z})$ is an optimal approximation of any value of $X = f(\mathbf{z}, U)$, with $\mathbf{Z} \perp\!\!\!\perp U$, we have the mean function as

$$\begin{aligned}\mu_\phi(\mathbf{z}) &= \mathbb{E}[X(\mathbf{z}, U)] = \int (f_a(\mathbf{z}) + f_b(\mathbf{z})f_c(u))p(u)du \\ &= f_a(\mathbf{z}) + \int f_b(\mathbf{z})f_c(u)p(u)du \\ &= f_a(\mathbf{z}) + f_b(\mathbf{z})\mathbb{E}[f_c(U)].\end{aligned}$$

Then with $U = u$,

$$\begin{aligned}x - \mu_\phi(\mathbf{z}) &= f_a(\mathbf{z}) + f_b(\mathbf{z})f_c(u) - f_a(\mathbf{z}) - f_b(\mathbf{z})\mathbb{E}[f_c(U)] \\ &= f_b(\mathbf{z})(f_c(u) - \mathbb{E}[f_c(U)]).\end{aligned}\tag{8}$$

With (8), the variance of regression model $\phi()$ is

$$\begin{aligned}\mathbb{E}[(X - \mu_\phi(\mathbf{z}))^2] &= \mathbb{E}\left[f_b(\mathbf{z})(f_c(U) - \mathbb{E}[f_c(U)])^2 f_b(\mathbf{z})\right] \\ &= f_b^2(\mathbf{z})\mathbb{E}\left[(f_c(U) - \mathbb{E}[f_c(U)])^2\right] \\ &= f_b^2(\mathbf{z})\sigma_{f_c}^2.\end{aligned}$$

As $\mathbf{Z} \perp\!\!\!\perp U$, as a function of \mathbf{Z} , the learned variance $\sigma_\phi^2(\mathbf{z})$ does not capture the information of U . $\sigma_\phi^2(\mathbf{z})$ learns the variance function with respect to variable \mathbf{Z} , i.e., $f_b^2(\mathbf{z})$. Therefore, $\sigma_\phi(\mathbf{z}) = c|f_b(\mathbf{z})|$. Then, by (8),

$$\begin{aligned}\frac{x - \mu_\phi(\mathbf{z})}{\sigma_\phi(\mathbf{z})} &= \frac{f_b(\mathbf{z})(f_c(u) - \mathbb{E}[f_c(U)])}{c|f_b(\mathbf{z})|} \\ &= \frac{s}{c}(f_c(u) - \mathbb{E}[f_c(U)]).\end{aligned}\tag{9}$$

Here $s = \text{sign}[f_b(\mathbf{z})]$. Let $a = \frac{s}{c}$, we define

$$\hat{U} := \frac{X - \mu_\phi(\mathbf{Z})}{\sigma_\phi(\mathbf{Z})} = a(f_c(U) - \mathbb{E}[f_c(U)]).$$

It shows that $\mathbb{E}[\hat{U}] = 0$, and $\hat{U} \perp\!\!\!\perp \mathbf{Z}$. □

It is easy to show that a τ -SCM with a decomposable $f()$ is counterfactually identifiable. Hence, Theorem 4.1 presents a new family of τ -SCMs that are counterfactually identifiable beyond BGMs (Bijective Generation Mechanisms, [16]).

B.2 Proof of Theorem 4.2

In this section, we present the proof of Theorem 4.2, and the proof is based on the analysis in [16; 17; 14]. We first present a lemma on the BGM equivalence class of a τ -SCM with a monotonic mechanism.

Lemma B.2. *Let (\mathbf{Z}, U, X, f) be a τ -SCM. $\forall \mathbf{z} \in \mathcal{Z}$, $f(\mathbf{z}, \cdot)$ is differentiable and strictly monotonic regarding $u \in \mathcal{U}$. We define a differentiable and invertible encoder function $h(\cdot) : \mathcal{Z} \times \mathcal{X} \rightarrow \hat{\mathcal{U}}$, i.e., $\hat{U} := h(\mathbf{Z}, X)$, and $\hat{U} \perp\!\!\!\perp \mathbf{Z}$. The decoder is $g(\cdot) : \mathcal{Z} \times \hat{\mathcal{U}} \rightarrow \mathcal{X}$, i.e., $X = g(\mathbf{Z}, \hat{U})$. Then $\hat{U} = h(\mathbf{Z}, X)$ is a function of U , i.e., $\hat{U} = \mathbf{s}(U)$, and $\mathbf{s}(\cdot)$ is an invertible function.*

Proof. According to the definition of τ -SCM, we have $\mathbf{Z} \perp\!\!\!\perp U$. According to the assumption, $\forall \mathbf{z} \in \mathcal{Z}$, $f(\mathbf{z}, u)$ is differentiable and strictly monotonic regarding u . Hence $X = f(\mathbf{Z}, U)$ is a BGM, and we use \mathbb{F} to represent BGM class that satisfies the independence ($\mathbf{Z} \perp\!\!\!\perp U$) and the function monotone conditions. We can see that $h^{-1} \in \mathbb{F}$, $h^{-1}(\mathbf{z}, \cdot) = g(\mathbf{z}, \cdot)$, and $h^{-1}(\mathbf{z}, \cdot)$ and $f(\mathbf{z}, \cdot)$ are counterfactually equivalent BGMs that generate the same distribution $p(\mathbf{Z}, X)$. Based Lemma B.2, Proposition 6.2, and Definition 6.1 in [16], there exists an invertible function $\mathbf{s}(\cdot)$ that satisfies $\forall \mathbf{z} \in \mathcal{Z}, x \in \mathcal{X}, h(\mathbf{z}, x) = \mathbf{s}(f^{-1}(\mathbf{z}, x))$, i.e., $\hat{u} = h(\mathbf{z}, x) = \mathbf{s}(f^{-1}(\mathbf{z}, x)) = \mathbf{s}(u)$, which is $\hat{U} = \mathbf{s}(U)$. \square

We can easily prove that an EDS model of a monotonic τ -SCM belongs to its BGM equivalence class under the independence assumption $\hat{U} \perp\!\!\!\perp \mathbf{Z}$.

Theorem 4.2 *Let (\mathbf{Z}, U, X, f) be a τ -SCM. $\forall \mathbf{z} \in \mathcal{Z}$, $f(\mathbf{z}, \cdot)$ is differentiable and strictly monotonic regarding $u \in \mathcal{U}$. Let (\hat{U}, ϕ, h, g) be an EDS surrogate of U . We further assume that $\hat{U} \perp\!\!\!\perp \mathbf{Z}$. Then $\hat{U} = h(\mathbf{Z}, X)$ is a function of U , i.e., $\hat{U} = \mathbf{s}(U)$, and $\mathbf{s}(\cdot)$ is an invertible function.*

Proof. It is to prove that the encoder of an EDS, i.e., $\hat{U} = h(\mathbf{Z}, X) = \frac{X - \mu_\phi(\mathbf{Z})}{\sigma_\phi(\mathbf{Z})}$, is invertible regarding \hat{U} and X given a value of \mathbf{Z} . With the assumption $\hat{U} \perp\!\!\!\perp \mathbf{Z}$, by using the results of Lemma B.2, we have $\hat{U} = h(\mathbf{Z}, X)$ is a function of U , i.e., $\hat{U} = \mathbf{s}(U)$, and $\mathbf{s}(\cdot)$ is an invertible function. \square

Based on the proof of Theorem 4.2, a τ -SCM with a monotonic mechanism is counterfactually identifiable by using an EDS model with the $\hat{U} \perp\!\!\!\perp \mathbf{Z}$ constraint.

C Regret Analysis

Our analysis follows the study in [23]. In the DAG \mathcal{G} over $\{X_i\}_0^d$, let N be the maximum distance from a root to X_d , i.e., $N = \max_i \text{dist}(X_i, X_d)$. Here $\text{dist}(\cdot, \cdot)$ is a measure of the edges in the longest path from X_i to the reward node X_d . Let M denote the maximum number of parents of any variables in \mathcal{G} , $M = \max_i |\text{pa}(i)|$. Let L_t be a function of L_g, L_{σ_g} . According to Theorem 4.1 and Theorem 4.2, with the EDS structure given in Figure 2 in the main text, the exogenous variable and its distribution can be recovered. For each observation of the dynamic surrogate model, we assume the sampling of $p(\hat{U})$, $\hat{u} = \mathbf{s}(\hat{u}) = \mathbf{s}(u)$.

We first give the assumptions used in the regret analysis. Assumption C.1 gives the Lipschitz conditions of g_i , $\sigma_{g,i}$, and $\mu_{g,i}$. It holds if the RKHS of each g_i has a Lipschitz continuous kernel [10; 23]. Assumption C.3 holds when we assume that the i th GP prior uses the same kernel as the RKHS of g_i and that $\beta_{i,t}$ is sufficiently large to ensure the confidence bounds in

$$\left| g_i(\mathbf{z}_i, a_i, \hat{u}_i) - \mu_{g,i,t-1}(\mathbf{z}_i, a_i, \hat{u}_i) \right| \leq \beta_{i,t} \sigma_{g,i,t-1}(\mathbf{z}_i, a_i, \hat{u}_i), \quad \forall \mathbf{z}_i \in \mathcal{Z}_i, a_i \in \mathcal{A}_i, \hat{u}_i \in \hat{\mathcal{U}}_i.$$

Assumption C.1. $\forall g_i \in \mathbf{G}$, g_i is L_g -Lipschitz continuous; moreover, $\forall i, t$, $\mu_{g,i,t}$ and $\sigma_{g,i,t}$ are L_{μ_g} and L_{σ_g} Lipschitz continuous.

Assumption C.2. $\forall f_i \in \mathbf{F}$, f_i is differentiable and has a decomposable structure with $X = f_i(\mathbf{Z}_i, U_i) = f_{i(a)}(\mathbf{Z}_i) + f_{i(b)}(\mathbf{Z}_i)f_{i(c)}(U_i)$, and $f_{i(b)}(\mathbf{z}_i) \neq 0, \forall \mathbf{z}_i \in \mathcal{Z}_i$.

Assumption C.3. $\forall i, t$, there exists sequence $\beta_{i,t} \in \mathbb{R}_{>0}$, with probability at least $(1 - \alpha)$, for all $\mathbf{z}_i, a_i, \hat{u}_i \in \mathcal{Z}_i \times \mathcal{A}_i \times \hat{\mathcal{U}}_i$ we have $|g_i(\mathbf{z}_i, a_i, \hat{u}_i) - \mu_{g,i,t-1}(\mathbf{z}_i, a_i, \hat{u}_i)| \leq \beta_{i,t}\sigma_{g,i,t-1}(\mathbf{z}_i, a_i, \hat{u}_i)$, and $|h(\mathbf{z}_i, a_i, x_i) - \mu_{h,i,t-1}(\mathbf{z}_i, a_i, x_i)| \leq \beta_{i,t}\sigma_{h,i,t-1}(\mathbf{z}_i, a_i, x_i)$.

The following lemma bounds the value of \tilde{u} with the variance of the encoder.

Lemma C.1.

$$\|\hat{u}_{i,t} - \tilde{u}_{i,t}\| \leq 2\beta_t \|\sigma_{\hat{u}_{i,t-1}}\| = 2\beta_t \|\sigma_{h,i,t-1}\|.$$

Proof. With Assumption C.3 and $\hat{u}_{i,t} = h_{i,i-1}(\mathbf{z}_i, a_i, x_i)$, let $\tilde{u}_{i,t} = \mu_{\hat{u}_{i,t-1}}(\mathbf{z}_i, a_i, x_i) + \beta_t \sigma_{\hat{u}_{i,t-1}}(\mathbf{z}_i, a_i, x_i) \circ \omega_{\hat{u}_{i,t-1}}(\mathbf{z}_i, a_i, x_i)$, and here $|\omega_{\hat{u}_{i,t-1}}(\mathbf{z}_i, a_i, x_i)| \leq 1$. Then

$$\begin{aligned} \|\hat{u}_{i,t} - \tilde{u}_{i,t}\| &= \|\hat{u}_{i,t} - \mu_{\hat{u}_{i,t-1}}(\mathbf{z}_i, a_i, x_i) - \beta_t \sigma_{\hat{u}_{i,t-1}}(\mathbf{z}_i, a_i, x_i) \circ \omega_{\hat{u}_{i,t-1}}(\mathbf{z}_i, a_i, x_i)\| \\ &\leq \|\hat{u}_{i,t} - \mu_{\hat{u}_{i,t-1}}(\mathbf{z}_i, a_i, x_i)\| + \beta_t \|\sigma_{\hat{u}_{i,t-1}}(\mathbf{z}_i, a_i, x_i) \circ \omega_{\hat{u}_{i,t-1}}(\mathbf{z}_i, a_i, x_i)\| \\ &\leq 2\beta_t \|\sigma_{\hat{u}_{i,t-1}}(\mathbf{z}_i, a_i, x_i)\| = 2\beta_t \|\sigma_{h,i,t-1}\|. \end{aligned}$$

□

With the decomposable Assumption C.2 on f_i , $\sigma_{h,i,t-1}^2 \propto f_{i(b)}^2(\mathbf{z}_i, a_i)(f_{i(c)}(U) - \mathbb{E}[f_{i(c)}(U)])^2$ according to the proof of Theorem 4.1. $f_{i(b)}()$ is learned with the variance of regression model $\phi()$, i.e. $\sigma_{\phi,i,t}()$.

Lemma C.2.

$$\|x_{d,t} - \tilde{x}_{d,t}\| \leq 2\beta_t M^{N_i} (2\beta_t L_{\sigma_g} + L_g)^{N_i} \sum_{j=0}^i (\sigma_{g,j,t-1}(\mathbf{z}_{j,t}) + \sigma_{\hat{u}_{j,t-1}}).$$

Proof. We use $g_i(\mathbf{z}_{i,t}, \hat{u}_{i,t})$ to represent $g_i(\mathbf{z}_{i,t}, a_{i,t}, \hat{u}_{i,t})$ because we assume the actions to be the same for the process generating $x_{i,t}$ and $\tilde{x}_{i,t}$. Similarly, $\mu_{g,i,t-1}(\tilde{\mathbf{z}}_{i,t}, \tilde{u}_{i,t}) = \mu_{g,i,t-1}(\tilde{\mathbf{z}}_{i,t}, \tilde{a}_{i,t}, \tilde{u}_{i,t})$, $\sigma_{g,i,t-1}(\tilde{\mathbf{z}}_{i,t}, \tilde{u}_{i,t}) = \sigma_{g,i,t-1}(\tilde{\mathbf{z}}_{i,t}, \tilde{a}_{i,t}, \tilde{u}_{i,t})$.

We use the reparameterization trick, and write $\tilde{x}_{i,t}$ as

$$\tilde{x}_{i,t} = \tilde{g}_i(\tilde{\mathbf{z}}_{i,t}, \tilde{u}_{i,t}) = \mu_{g,i,t-1}(\tilde{\mathbf{z}}_{i,t}, \tilde{u}_{i,t}) + \beta_t \sigma_{g,i,t-1}(\tilde{\mathbf{z}}_{i,t}, \tilde{u}_{i,t}) \circ \omega_{g,i,t-1}(\tilde{\mathbf{z}}_{i,t}, \tilde{u}_{i,t}).$$

Here $|\omega_{g,i,t-1}(\tilde{\mathbf{z}}_i, \tilde{u}_{i,t})| \leq 1$. Hence, we have

$$\begin{aligned}
\|x_{i,t} - \tilde{x}_{i,t}\| &= \|g_i(\mathbf{z}_{i,t}, \hat{u}_{i,t}) - \mu_{g,i,t-1}(\tilde{\mathbf{z}}_i, \tilde{u}_{i,t}) - \beta_t \sigma_{g,i,t-1}(\tilde{\mathbf{z}}_i, \tilde{u}_{i,t}) \omega_{g,i,t-1}(\tilde{\mathbf{z}}_i, \tilde{u}_{i,t})\| \\
&= \|g_i(\tilde{\mathbf{z}}_i, \tilde{u}_{i,t}) - \mu_{g,i,t-1}(\tilde{\mathbf{z}}_i, \tilde{u}_{i,t}) - \beta_t \sigma_{g,i,t-1}(\tilde{\mathbf{z}}_i, \tilde{u}_{i,t}) \omega_{g,i,t-1}(\tilde{\mathbf{z}}_i, \tilde{u}_{i,t}) \\
&\quad + g_i(\mathbf{z}_{i,t}, \hat{u}_{i,t}) - g_i(\tilde{\mathbf{z}}_i, \tilde{u}_{i,t})\| \\
&\leq \|g_i(\tilde{\mathbf{z}}_i, \tilde{u}_{i,t}) - \mu_{g,i,t-1}(\tilde{\mathbf{z}}_i, \tilde{u}_{i,t})\| + \|\beta_t \sigma_{g,i,t-1}(\tilde{\mathbf{z}}_i, \tilde{u}_{i,t}) \omega_{g,i,t-1}(\tilde{\mathbf{z}}_i, \tilde{u}_{i,t})\| \\
&\quad + \|g_i(\mathbf{z}_{i,t}, \hat{u}_{i,t}) - g_i(\tilde{\mathbf{z}}_i, \tilde{u}_{i,t})\| \\
&\stackrel{\zeta_1}{\leq} \beta_t \|\sigma_{g,i,t-1}(\tilde{\mathbf{z}}_i, \tilde{u}_{i,t})\| + \beta_t \|\sigma_{g,i,t-1}(\tilde{\mathbf{z}}_i, \tilde{u}_{i,t})\| + L_{g_i} \|\mathbf{z}_{i,t}; \hat{u}_{i,t}\| - [\tilde{\mathbf{z}}_i, \tilde{u}_{i,t}] \\
&= 2\beta_t \|\sigma_{g,i,t-1}(\mathbf{z}_i, \hat{u}_{i,t}) + \sigma_{g,i,t-1}(\tilde{\mathbf{z}}_i, \tilde{u}_{i,t}) - \sigma_{g,i,t-1}(\mathbf{z}_i, \hat{u}_{i,t})\| + L_{g_i} \|\mathbf{z}_{i,t}; \hat{u}_{i,t}\| - [\tilde{\mathbf{z}}_i, \tilde{u}_{i,t}] \\
&\stackrel{\zeta_2}{\leq} 2\beta_t \left(\|\sigma_{g,i,t-1}(\mathbf{z}_i, \hat{u}_{i,t})\| + L_{\sigma_{g,i}} \|\mathbf{z}_{i,t}; \hat{u}_{i,t}\| - [\tilde{\mathbf{z}}_i, \tilde{u}_{i,t}] \right) + L_{g_i} \|\mathbf{z}_{i,t}; \hat{u}_{i,t}\| - [\tilde{\mathbf{z}}_i, \tilde{u}_{i,t}] \\
&= 2\beta_t \sigma_{g,i,t-1}(\mathbf{z}_i, \hat{u}_{i,t}) + (2\beta_t L_{\sigma_{g,i}} + L_{g_i}) \|\mathbf{z}_{i,t}; \hat{u}_{i,t}\| - [\tilde{\mathbf{z}}_i, \tilde{u}_{i,t}] \\
&\leq 2\beta_t \sigma_{g,i,t-1}(\mathbf{z}_i, \hat{u}_{i,t}) + (2\beta_t L_{\sigma_{g,i}} + L_{g_i}) \|\mathbf{z}_{i,t} - \tilde{\mathbf{z}}_i\| + (2\beta_t L_{\sigma_{g,i}} + L_{g_i}) \|\hat{u}_{i,t} - \tilde{u}_{i,t}\| \\
&\stackrel{\zeta_3}{\leq} 2\beta_t \sigma_{g,i,t-1}(\mathbf{z}_i, \hat{u}_{i,t}) + (2\beta_t L_{\sigma_{g,i}} + L_{g_i}) \|\mathbf{z}_{i,t} - \tilde{\mathbf{z}}_i\| + 2\beta_t (2\beta_t L_{\sigma_{g,i}} + L_{g_i}) \sigma_{\hat{u}_{i,t-1}} \\
&= 2\beta_t \sigma_{g,i,t-1}(\mathbf{z}_i, \hat{u}_{i,t}) + 2\beta_t (2\beta_t L_{\sigma_{g,i}} + L_{g_i}) \sigma_{\hat{u}_{i,t-1}} + (2\beta_t L_{\sigma_{g,i}} + L_{g_i}) \sum_{j \in \text{pa}(i)} \|\mathbf{z}_{j,t} - \tilde{\mathbf{z}}_{j,t}\| \\
&\leq 2\beta_t \sigma_{g,i,t-1}(\mathbf{z}_i, \hat{u}_{i,t}) + 2\beta_t (2\beta_t L_{\sigma_g} + L_g) \sigma_{\hat{u}_{i,t-1}} + (2\beta_t L_{\sigma_g} + L_g) \sum_{j \in \text{pa}(i)} \|x_{j,t} - \tilde{x}_{j,t}\| \\
&\stackrel{\zeta_4}{\leq} 2\beta_t \sigma_{g,i,t-1}(\mathbf{z}_i, \hat{u}_{i,t}) + 2\beta_t (2\beta_t L_{\sigma_g} + L_g) \sigma_{\hat{u}_{i,t-1}} \\
&\quad + (2\beta_t L_{\sigma_g} + L_g) \sum_{j \in \text{pa}(i)} 2\beta_t M^{N_j} (2\beta_t L_{\sigma_g} + L_g)^{N_j} \sum_{h=0}^j (\sigma_{g,h,t-1}(\mathbf{z}_{h,t}) + \sigma_{\hat{u}_{h,t-1}}) \\
&\leq 2\beta_t M^{N_i} (2\beta_t L_{\sigma_g} + L_g)^{N_i} \sum_{j=0}^i (\sigma_{g,j,t-1}(\mathbf{z}_{j,t}) + \sigma_{\hat{u}_{j,t-1}})
\end{aligned}$$

In steps ζ_1 and ζ_2 , we rely on the calibrated uncertainty and Lipschitz dynamics; in step ζ_2 , we also apply the triangle inequality; step ζ_3 is by Lemma C.1; ζ_4 applies the inductive hypothesis. \square

Theorem 6.1 Consider the optimization problem in (4), with the SCM satisfying Assumptions C.1-C.3, where \mathcal{G} is known but \mathbf{F} is unknown. Then with probability at least $1 - \alpha$, the cumulative regret of Algorithm 1 is bounded by

$$R_T \leq \mathcal{O}(L_T M^N d \sqrt{T \gamma_T}).$$

Proof. The cumulative regret is

$$R_T = \sum_{t=1}^T \left[\mathbb{E}[y|\mathbf{a}^*] - \mathbb{E}[y|\mathbf{a}_{:,t}] \right].$$

At step t , the instantaneous regret is r_t . By applying Lemma C.2, r_t is bounded by

$$\begin{aligned}
r_t &= \mathbb{E}[y|\mathbf{F}, \mathbf{a}^*] - \mathbb{E}[y|\mathbf{F}, a_{:,t}] \\
&\leq \mathbb{E}[y_t|\tilde{\mathbf{F}}, a_{:,t}] - \mathbb{E}[y_t|\mathbf{F}, a_{:,t}] \\
&= \mathbb{E}[\|x_{i,t} - \tilde{x}_{i,t}\| | a_{:,t}] \\
&\leq 2\beta_t M^N (2\beta_t L_{\sigma_g} + L_g)^N \mathbb{E} \left[\sum_{i=0}^d \|\sigma_{g,i,t-1}(\mathbf{z}_{i,t})\| + \|\sigma_{\hat{u}_{i,t-1}}\| \right]
\end{aligned}$$

Here $L_t = 2\beta_t(2\beta_t L_{\sigma_g} + L_g)^N$. Thus,

$$\begin{aligned}
r_t^2 &\leq L_t^2 M^{2N} \left(\mathbb{E} \left[\sum_{i=0}^d \|\sigma_{g,i,t-1}(\mathbf{z}_{i,t})\| + \|\sigma_{\hat{u}_{i,t-1}}\| \right] \right)^2 \\
&\leq 2dL_t^2 M^{2N} \mathbb{E} \left[\sum_{i=0}^d \|\sigma_{g,i,t-1}(\mathbf{z}_{i,t})\|_2^2 + \|\sigma_{\hat{u}_{i,t-1}}\|_2^2 \right]
\end{aligned}$$

We define R_T^2 as

$$\begin{aligned}
R_T^2 &= \left(\sum_{t=1}^T r_t \right)^2 \leq T \sum_{t=1}^T r_t^2 \\
&\leq 2dT L_T^2 M^{2N} \sum_{t=1}^T \mathbb{E} \left[\sum_{i=0}^d \|\sigma_{g,i,t-1}(\mathbf{z}_{i,t})\|_2^2 + \|\sigma_{\hat{u}_{i,t-1}}\|_2^2 \right] \\
&= 2dT L_T^2 M^{2N} \Gamma_T.
\end{aligned}$$

Here,

$$\begin{aligned}
\Gamma_T &= \max_{(\mathbf{z}, a, \hat{u}) \in \mathcal{Z} \times \mathcal{A} \times \hat{\mathcal{U}}} \sum_{t=1}^T \sum_{i=0}^d \left[\|\sigma_{i,t-1}(\mathbf{z}_{i,t}, a_{i,t})\|_2^2 + \|\sigma_{\hat{u}_{i,t-1}}\|_2^2 \right] \\
&\leq \max_{A, \hat{U}} \sum_{t=1}^T \sum_{i=0}^d \left[\|\sigma_{i,t-1}(\mathbf{z}_{i,t}, a_{i,t})\|_2^2 + \|\sigma_{\hat{u}_{i,t-1}}\|_2^2 \right] \\
&\leq \sum_{i=0}^d \max_{A_i, \hat{U}_i} \sum_{t=1}^T \left[\|\sigma_{i,t-1}(\mathbf{z}_{i,t}, a_{i,t})\|_2^2 + \|\sigma_{\hat{u}_{i,t-1}}\|_2^2 \right] \\
&\leq \sum_{i=0}^d \max_{A_i, \hat{U}_i} \sum_{t=1}^T \left[\sum_{l=1}^{d_i} \|\sigma_{i,t-1}(\mathbf{z}_{i,t}, a_{i,t}, l)\|_2^2 + \|\sigma_{\hat{u}_{i,t-1}}\|_2^2 \right] \\
&\leq \sum_{i=0}^d \frac{2}{\ln(1 + \rho_i^{-2})} \gamma_{i,T} \\
&= \mathcal{O}(d\gamma_T).
\end{aligned}$$

Here ζ_1 is due to the upper bound of the information gain [21], and γ_T will often scale sublinearly in T [23]. Therefore,

$$R_T^2 \leq 2dT L_T^2 M^{2N} d\mathcal{O}(d\gamma_T).$$

And,

$$R_T \leq \mathcal{O}(L_T M^N d \sqrt{T \gamma_T}).$$

This completes the proof of the theorem. □

D Additional Experimental Results

D.1 Dropwave Dataset

The structure of Dropwave is given in Figure 7. Figure 8 gives the average reward values achieved by the competing algorithms using four different random seeds in the code, and shadows are the scaled standard deviations of the four results. In each round, the size of the observation on the true model equals the round number.

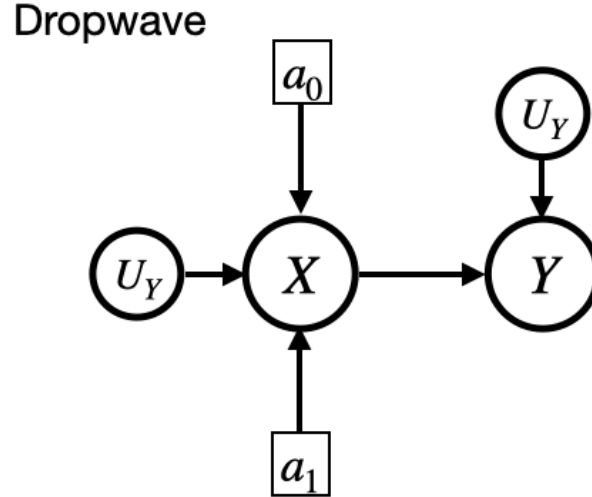
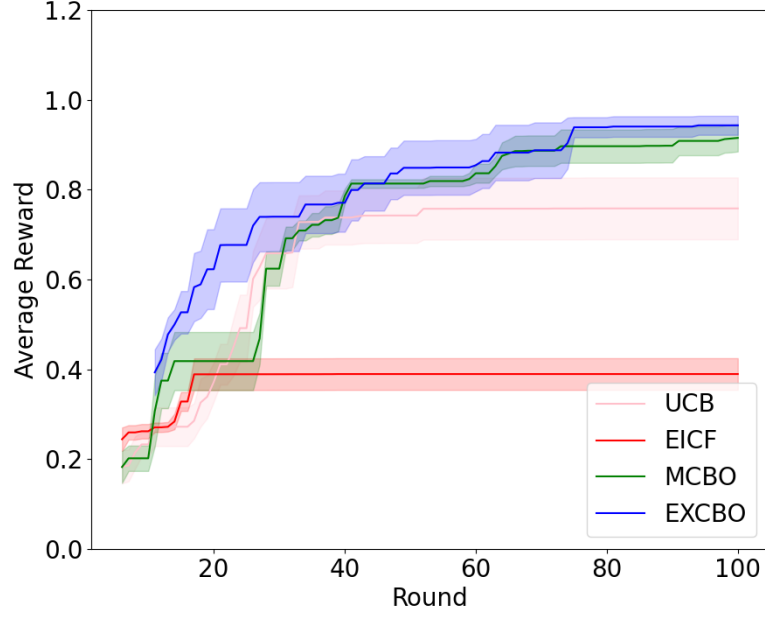


Figure 7: Graph structure of Dropwave dataset.

(a) $\sigma = 0.05$



(b) $\sigma = 0.3$

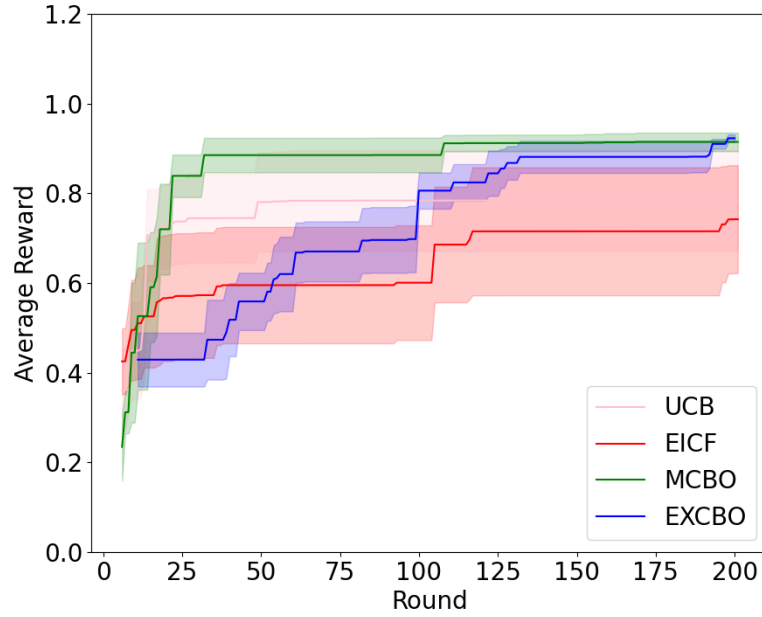


Figure 8: Results of Dropwave at different noise levels.

Figure 8-(a) presents the results at $\sigma = 0.05$. It can be observed clearly that EXCBO achieves the best reward at nearly all rounds. Figure 8-(b) gives the results at $\sigma = 0.3$. In Figure 8-(b),

EXCBO exceeds UCB and EICF at round 130, and it achieves the best performance at round 193. It indicates that our EXCBO method may require more training samples to recover the exogenous distribution especially when the variance of the noise is large.

Empirically, the proposed EXCBO uses a similar CPU time as UCB for the same round number on different datasets. EICF takes a little bit more computational cost compared to EXCBO and UCB. However, MCBO consumes much more CPU time (10+ times) compared to the other three methods that do not rely on neural networks. This means that EXCBO is more scalable in terms of computational cost in comparison with the existing state-of-the-art methods.

D.2 Additional Experimental Analysis on EXCBO

This section presents an additional empirical analysis of the proposed EXCBO algorithm.

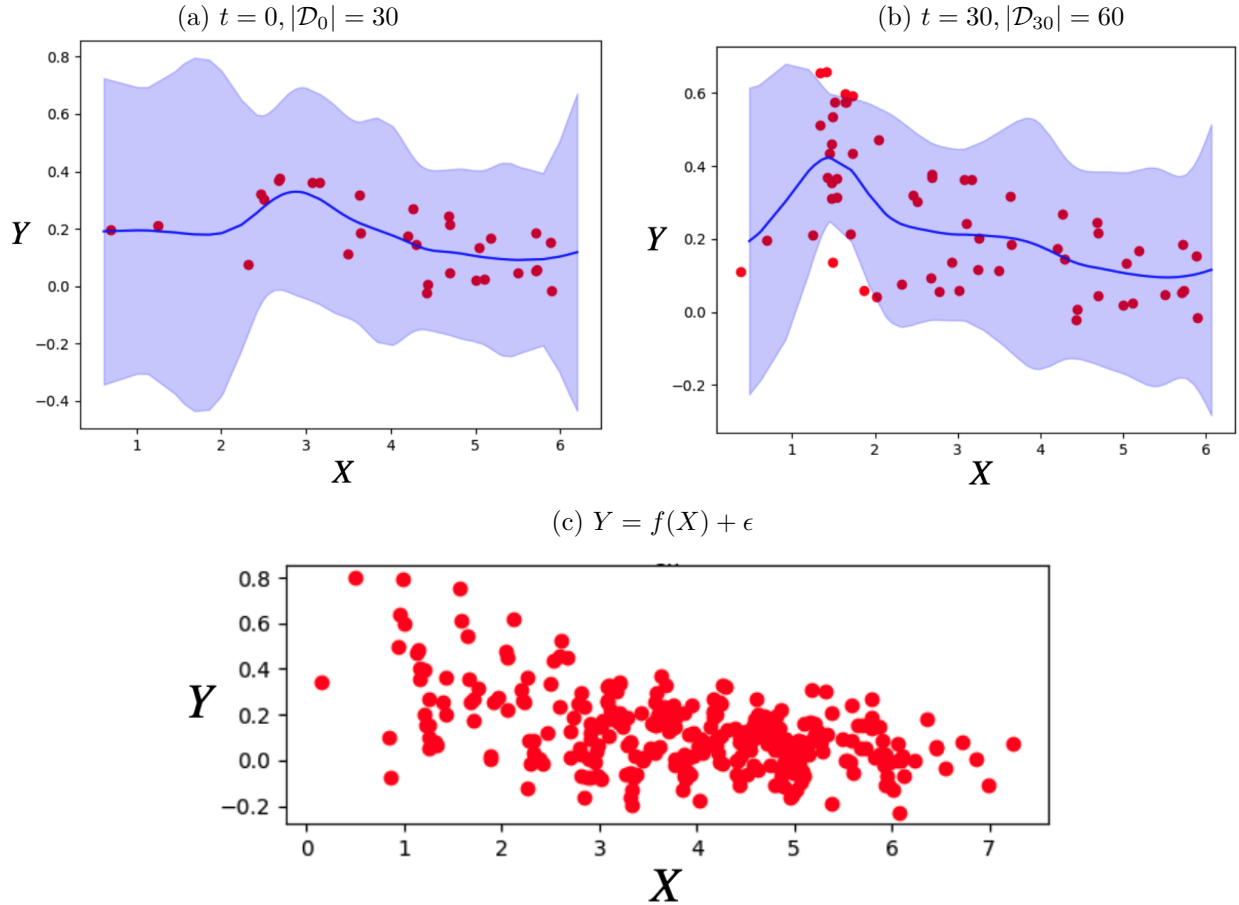


Figure 9: Surrogate model of EXCBO on Dropwave. The blue curve is the surrogate mean, and the blue shadow stands for the scaled standard derivation of the surrogate model; red points are samples from the ground truth model. (a) At step $t = 0$, the model is initialized with 30 samples; (b) At step $t = 30$, more observations are around the optimal location; (c) Samples from the ground truth function of Y .

Dropwave Dataset

The graph structure of the Dropwave Dataset is given by Figure 7. There are two endogenous nodes in Dropwave, i.e., X and the target node Y . There are two action nodes associated with X , a_0 and a_1 . Here $a_0, a_1 \in [0, 1]$, $X = \sqrt{(c_1 \cdot a_0 - c_2)^2 + (c_1 \cdot a_1 - c_2)^2} + \epsilon_X$, $c_1 = 10.24$, $c_2 = 5.12$,

and $Y = (1.0 + \cos(12.0X))/(2.0 + 0.5X^2) + \epsilon_Y$, $\epsilon_X, \epsilon_Y \sim \mathcal{N}(0, \sigma)$. We change the value of σ to generate data samples with different noise levels.

We performed a further investigation on the surrogate model learned by the EXCBO algorithm using the Dropwave dataset at $\sigma = 0.1$. The algorithm is initialized with 30 data samples, and then we plot the learned surrogate function from X and Y at step $t = 30$. Figure 9 shows the surrogate model mean and scaled standard deviation at $t = 0$ and $t = 30$. Plot (c) in Figure 9 shows the data points sampled from the ground truth model, and it indicates that the dataset is very noisy. As shown in the plots, at $t = 0$ data points are evenly sampled in the value span of X . At $t = 30$, we can see that the probabilistic surrogate model drives the EXCBO algorithm to obtain more samples around the optimal location. We further notice that the variance of the surrogate decreases at the locations with dense data samples. Plots (a) and (b) show that the surrogate model employed by EXCBO improves the learning of the unknown function as well as the estimation of uncertainty along with more observations.

Rosenbrock Dataset

Figure 10 shows the graph structure of the Rosenbrock dataset. Figure 11 shows the average reward values attained by the proposed EXCBO algorithm with nine different random seeds. The surrogate model is initialized with 20 samples. As shown in the figure, similar to Dropwave the reward values increase with more observational data points in the training set. However, different from the result of Dropwave, the variance of the reward value decreases significantly with more training data samples. Another difference from Dropwave is that the performance of the EXCBO algorithm is barely affected by the noise level in the dataset.

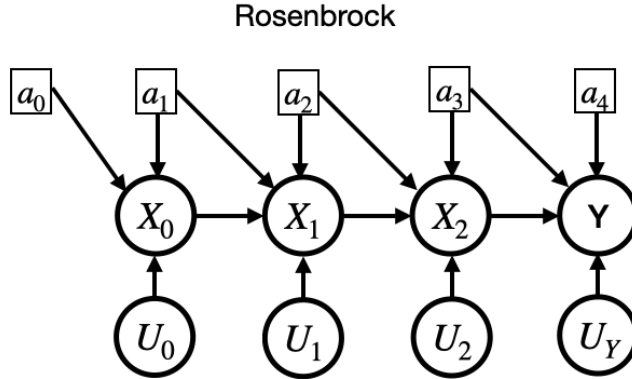


Figure 10: Graph structure of Rosenbrock dataset.

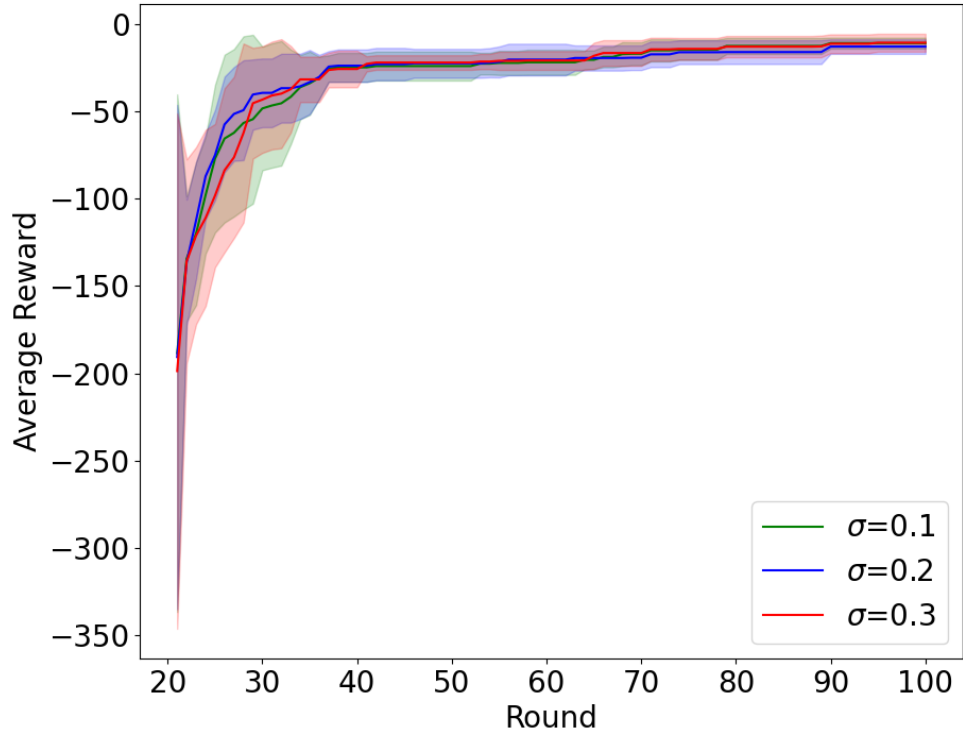


Figure 11: Reward values achieved by EXCBO in different rounds on Rosenbrock. The results are on three different Gaussian noise levels with $\sigma = \{0.1, 0.2, 0.3\}$.